Brazilian Journal of Geophysics

BrJG

Brazilian Journal of Geophysics 43 (2025), 2, 1-24
Brazilian Geophysical Society
ISSN 2764-8044
DOI: 10.22564/brjg.v43i2.2340

# A CASE STUDY OF 2-D SEISMIC REFRACTION TOMOGRAPHY AND REGULARIZATION EFFECTS, USING THE TIKHONOV APPROACH APPLIED TO SHALLOW MARINE ENVIRONMENT

Frank Cenci Bulhoes[1*], Luiz Alberto Santos[1,2], Marco Cetale[2], and Victor Thadeu Xavier de Almeida[1]

[1]Petrobras – Petróleo Brasileiro S.A., Rio de Janeiro, RJ, Brazil
[2]Universidade Federal Fluminense - UFF, GISIS, Niterói, RJ, Brazil

*corresponding author email: frankcenci@petrobras.com.br

Bulhões, F. C.: 0000-0001-9197-3905
Santos, L. A.: 0000-0003-4782-0826
Cetale, M.: 0000-0001-8604-5389
de Almeida, V.T.X.: 0000-0003-1333-4707



**ABSTRACT.** A common approach to stabilize the ill-posed inverse problem is to apply regularization, which restricts the possible solutions to these problems. Thus, a regularization term is often incorporated into the tomographic objective function to resolve the non-uniqueness of the inverse geophysical problem, restricting the possible solutions to these problems. This work evaluates the effects of regularization and analyzes its impact on the resulting seismic velocities. Grounded in a detailed case study, we investigate Tikhonov's regularization of order 1 and its variants, including order 2, utilizing a tomography program that employs ray tracing, a finite differences scheme with the eikonal equation for first arrivals, and the regularization algorithm. The velocity model is synthetic and based on shallow seabed channel geology. The true model was compared with the tomography results without regularization and with regularization schemes. The results clearly indicate that regularization parameters play a critical role in defining the outcomes of velocity models in tomography inversion. By applying regularization, we significantly reduce structural distortion in tomographic results—this approach proves to be not only effective but essential. Tikhonov’s regularization of order 2 consistently demonstrates faster convergence and notable improvements in the velocity model. Furthermore, our parameter sensitivity tests reveal the extent to which an inappropriate choice can distort geological structures, such as by creating artificial structural highs or lows, underscoring the necessity of careful selection in regularization techniques.

**Keywords:** seismic velocity inversion; shallow subsurface imaging; tomographic inversion; regularization schemes; Ill-posed inverse problems

## INTRODUCTION

Most geophysical studies deal with inverse problems since the acquisition of direct measures of physical properties is costly. Also, forward measures are generally restricted to spatially limited areas and difficult to extrapolate to the entire area of interest with the necessary accuracy, even with the use of geostatistical methods.

In the geophysics of oil and gas exploration, seismic methods have been the most used since the beginning of the 20th century (Telford et al., 1990). At the end of the 20th century and the beginning of the 21st, there was a significant advance in the oil and gas industry with the large-scale use of 3-D seismic survey data. The increase in computational capacities has generated great advances, significantly impacting deep seismic processing (Woodward et al., 2008). In this way, seismic velocity models have become fundamental for seismic imaging (Rosa et al., 2018; Maul et al., 2018).

The two main techniques for the seismic method are reflection and refraction (Telford et al., 1990). As per these authors, seismic reflection uses the seismic wave reflected in interfaces of materials with distinct acoustic impedances (compressional velocity and density) to characterize the medium, and seismic refraction uses the critically refracted wave at these interfaces. The seismic method is the most widely used technique in the field today. A recent survey conducted by Bulhões and Santos (2022) in the Scopus database reveals that publications between 1889 and 2021, 80% of publications focus on reflection seismic, while only 20% concentrate on refraction seismic (Figure 1). From the 1980s onwards, publications and studies on reflection seismic became predominant about those on refraction seismic. These results are corroborated by the work of Dobecki and Romig (1985), where it was observed that surveys and studies on reflection seismic would replace those on refraction as the predominant method. This trend highlights the growing recognition and preference for reflection seismic in research and practice.

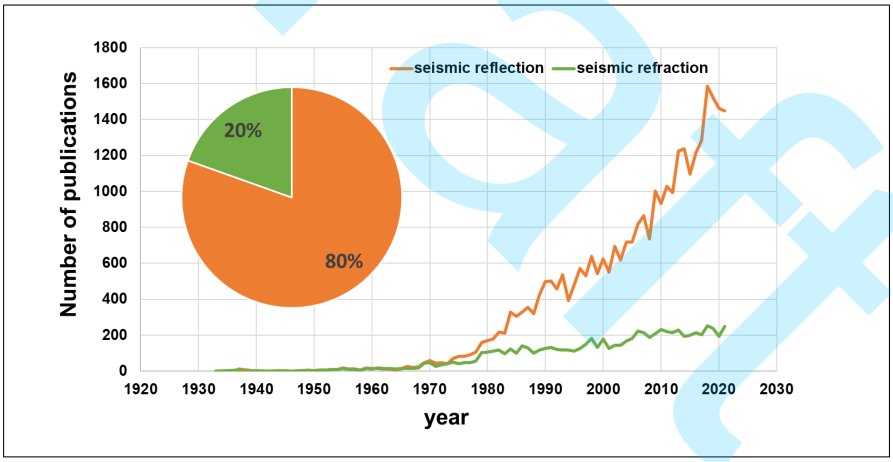


**Figure 1 -** Evolution of seismic works on reflection and refraction in relation to years. Adapted from Bulhões and Santos (2022).

The oil & gas industry's targets of interest are generally situated at great depths. Consequently, this fact imposes significant difficulties in reaching these targets by adopting refraction tomography. Furthermore, velocity models in shallow portions directly influence imaging and can lead to misinterpretation of deeper structures. In particular, static corrections used in onshore data processing depend heavily on the shallow velocity model, making it a primary source of uncertainties and errors. This dependency thus generates challenges for seismic processing (Lines and Newrick, 2004).

Due to the scarcity of information acquisition—specifically regarding feasible property distribution like compressional velocity — the characterization of the shallow subsurface remains a well-recognized challenge for exploration geophysics. The limited availability of this data in well logs, whether stemming from operational constraints or economic factors, underscores the complexity of the task. Nevertheless, information from the shallow portions of velocity models is crucial for seismic imaging and time-depth conversion in interpretation sectors.

Moreover, regularization is not merely a tool but necessary for solving seismic inversion problems (Zhdanov, 2002). The foundational works of Ivanov (1962), Phillips (1962), Twomey (1963) and Tikhonov (1963) established the groundwork for the general formulation of regularization in the context of ill-posed problems. Notably, the Tikhonov regularization technique — designed to ensure horizontal smoothness of geological properties — demonstrates the indispensable role of regularization in addressing geological challenges. The primary objective of this study is to evaluate the effects of regularization on refraction tomography and the resulting seismic velocities.

In addition, this research emerged from regional velocity modeling for time-depth conversion in basin scale. This was based on the methodology developed by Bulhões et al. (2014), which utilizes different types of seismic data. To get a robust velocity model, all available velocity information (tomography, migration, well profiles etc.) must be used, and weighted with geological information, statistical treatments, and geostatistical tools (Maul et al., 2005; Bulhões et al., 2018). However, in many cases, the shallow sections of wells remain unlogged due to operational instability and economic considerations (Bulhões et al., 2018). Figure 2 illustrates the seismic section of cross-reflection as observed in three wells alongside their respective sonic profiles.

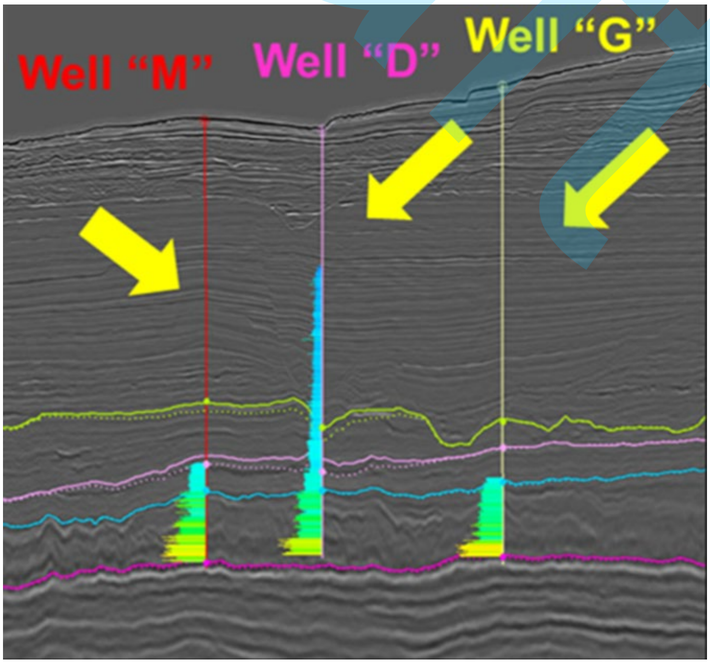


**Figure 2 -** Seismic section that passes through three wells and their respective sonic profiles. Adapted from Bulhões et al. (2018).

This work is split as follows: in the first part, a literature review on direct and inverse problems, as well as tomography and regularization, is presented. In the second part, it is shown an application of a case study in a shallow marine environment on the regularization of refraction tomography and its effects. Finally, the effects of Tikhonov regularizations as described in Tikhonov and Arsenin (1977) are evaluated.

## METHODS

### Forward and Inverse Problems

Menke (1989) defines an inverse problem as a collection of mathematical techniques that extract physical parameters from observed data. These techniques not only involve the creation of a physical-mathematical model that accurately represents the physical system but also justify the extracted parameters. Importantly, a problem is deemed inverse when the objective is to infer the physical properties of a medium based on external recorded data. Furthermore, a more comprehensive definition of an inverse problem encompasses understanding how to derive the physical model—a set of properties and parameters—from the observed data and corresponding observations. This process is frequently evident in various examples of geophysical and geological interpretation. By grasping these concepts, we can unlock a deeper understanding of the physical world, ultimately leading to more effective analyses and applications in these fields.

The linear inversion theory is expressed by:

$$\boldsymbol{d} = \boldsymbol{G}\boldsymbol{m} \qquad \text{Eq. 1}$$

Where:

**d** is the data vector corresponding to an observation;
**m** is the model parameter;
**G** is the matrix that relates the parameters **d** and **m**.

Figure 3 schematically shows forward and inverse problems. The inverse problem consists of having d and obtaining m. The forward problem is obtaining d from m and G.

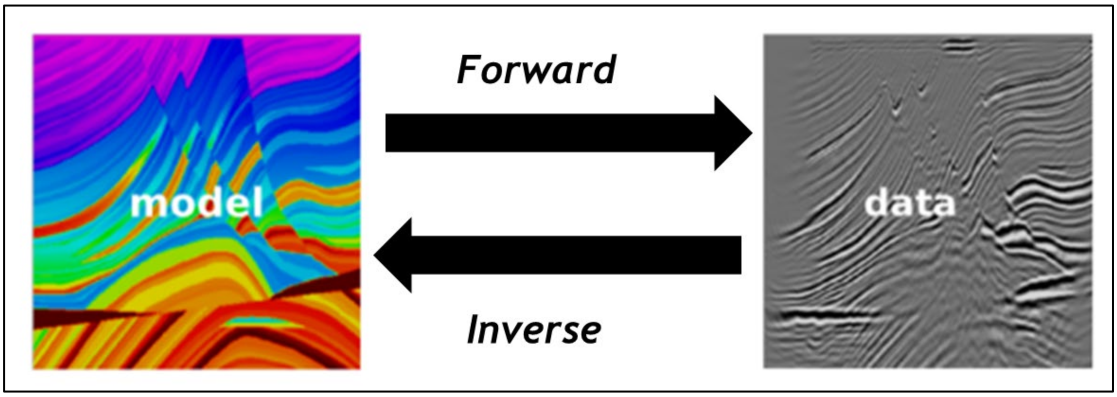


**Figure 3 -** Schematic representation of a forward and inverse problem. Adapted from Bianco (2013).

## Well-posed and Ill-posed Problems

Hadamard (1902) established that an inverse problem is called as ill-posed when the solution does not meet at least one of the conditions: existence, uniqueness, or stability. In a well-posed problem, the three conditions mentioned must be satisfied.

The uniqueness of the solution to inverse problems is crucial for classifying these problems as well-posed. Currently, inverse problems are often ill-posed, and it is imperative to transform them into well-posed problems by utilizing a priori information, regularizations, or other resources that restrict potential solutions effectively. According to Ivanov et al. (2005a), five main factors contribute to non-uniqueness, particularly evident in refraction tomography: insufficient data hampers the ability to resolve the problem effectively, especially in first-arrival tomography, where the model's cells often lack coverage by the rays, the intrinsic characteristics of the problem also play a significant role (in refraction tomography, blind layers, characterized by the lowest velocity in the deepest layers, prevent the rays from crossing these regions due to the medium's properties. - Data errors further complicate the situation; the statistical distribution of the data frequently deviates from Gaussian characteristics. This discrepancy means that the measured values might not accurately represent the model used for inversion; finally, numerical errors and instability can introduce significant challenges. These factors illuminate the challenges faced in executing refraction tomography. The non-uniqueness in first-arrival tomography clarifies why this method may lead to unsatisfactory solutions or, in some cases, total failure to produce results (Ivanov et al., 2005b). Achieving a satisfactory solution becomes highly improbable without incorporating the necessary a priori information. Hence, it is essential to address these issues to improve the reliability and effectiveness of inverse problems in practice

According to Zhdanov (2002), all information about the physical model (**m**) generates (**d**), according to Equation 1, is contained in matrix **G**. However, the presence of errors in the measured data, whether in the measurement, noise inherent in the system, or associated with the physical problem, poses a significant challenge. These imprecisions not considered in the modeling can exert difficulties to find out the correct model **m**, which accurately describes the registered data **d**. As Aster et al. (2005) point out, the possibility that the model adopted to describe the data is not correct (or complete) further complicates the task of obtaining a solution to the problem.

## Least Squares Method

The least squares method is a vital geophysical technique to determine the best-fit model parameters for inverse problems. This method seeks to achieve the smallest sum of squared residuals by minimizing the difference between observed and predicted data. It is particularly advantageous for overdetermined systems, where it allows for the identification of unique solutions that minimize overall errors (Claerbout and Muir, 1973). This method for curve fitting, while relatively sensitive to noise with very high amplitudes, is indispensable. The residual, the difference between the data calculated by direct modeling and the observed data, must be minimized and acceptable for the studied problem. Additionally, it can be applied to underdetermined systems, helping to find solutions closest to the observed data. The method includes linear least squares, which assume a linear relationship and offer a closed-form solution, and nonlinear least squares, which often require iterative approaches (Bejarano and Bassrei, 2016). In the case of the nonlinear problem, the widely used L2 norm aims to minimize the residual calculation function. The L2 norm, a standard method for calculating the length of a vector in Euclidean space (Li and Jain, 2009), plays a key role in this process.

The iterative process, a systematic and methodical approach, is the practice of refining and seeking to solve the problem described in Equation 1 through successive iterations. It starts from an initial model, and the problem is replaced by a sequence of linear least-squares problems, solved in subsequent iterations. The final solution converges to the solution of the original nonlinear problem (Heath, 2002; Menke, 2012). The process ends when the residual is less than a chosen minimum value ($\delta$) or when a maximum number of iterations (n) is reached (Zhdanov, 2002). When there are iterative methods for solving, it is necessary to define a convergence criterion. The criterion for convergence of the iterative process in this work is that the residual has a variation of less than 1% between iterations (Begnaud et al., 2013). Numerical methods must satisfy some interdependent: consistency, stability, or convergence. Consistency implies that the discrete problem approximates the differential problem. The solution found must converge to the solution of the equations when the distance between the mesh points tends to zero, i.e., when the solution of the discretized equations tends to the exact solution. A solution method is stable if the errors of the solution decrease, that is when it does not amplify the errors during the numerical simulation process (Ferziger and Peric, 1996). According to Lax's equivalence theorem, the method is convergent if only if it is stable. In this way, the methods need to have a numerical solution of finite difference methods of partial differential equations, a consistent finite difference method for a well-posed linear initial value problem. In other words, the relationship is true if consistency plus stability equals convergence. In nonlinear cases, convergence is not guaranteed. However, the method's stability substantially facilitates obtaining a converged solution (Tannehill et al., 1997).

The smaller residual of the data does not necessarily imply that the model's RMS error (i.e., the difference with models in subsequent steps) is smaller, especially if the problem is misplaced. In other words, the best fit between theoretical and observed times is the one for which the RMS is smaller. Thus, in the context of least squares, the objective function to be minimized is the square of the residual.

The problem is defined as nonlinear when the operator **G** is a function of the parameters of the model $\boldsymbol{m}$, (**d**=**g**(**m**)), the matrix **G** is an approximation of a nonlinear operator g. Tomography aims to obtain a velocity model that minimizes the objective function given by the difference between the travel times calculated in the forward modeling ($\boldsymbol{d_{calc}} = \mathbf{g}(\boldsymbol{m})$ ) and observed data ($\boldsymbol{d_{obs}}$ ), is expressed by:

$$\varphi(\boldsymbol{m}) = \|\boldsymbol{d_{obs}} - \boldsymbol{g}(\boldsymbol{m})\|_2{}^2 \quad \text{Eq. 2}$$

Where:

$\mathbf{d_{obs}}$ is the observed data; $\mathbf{g}$ ($\mathbf{m}$) is the calculated data.

According to Carbonesi (2018), the general workflow of tomographic inversion needs to contain as steps: the recorded data, the definition of an initial model for direct modeling, the definition of the number of iterations, n, and the misfit tolerance, δ; the calculation of the residual; if the residual is smaller than the tolerance the flow ends, otherwise the input model is updated by the parameter Δ**m** until either the residual is smaller than the tolerance or the number of predefined iterations is performed. Figure 4 shows the general workflow of tomographic inversion used in this study.

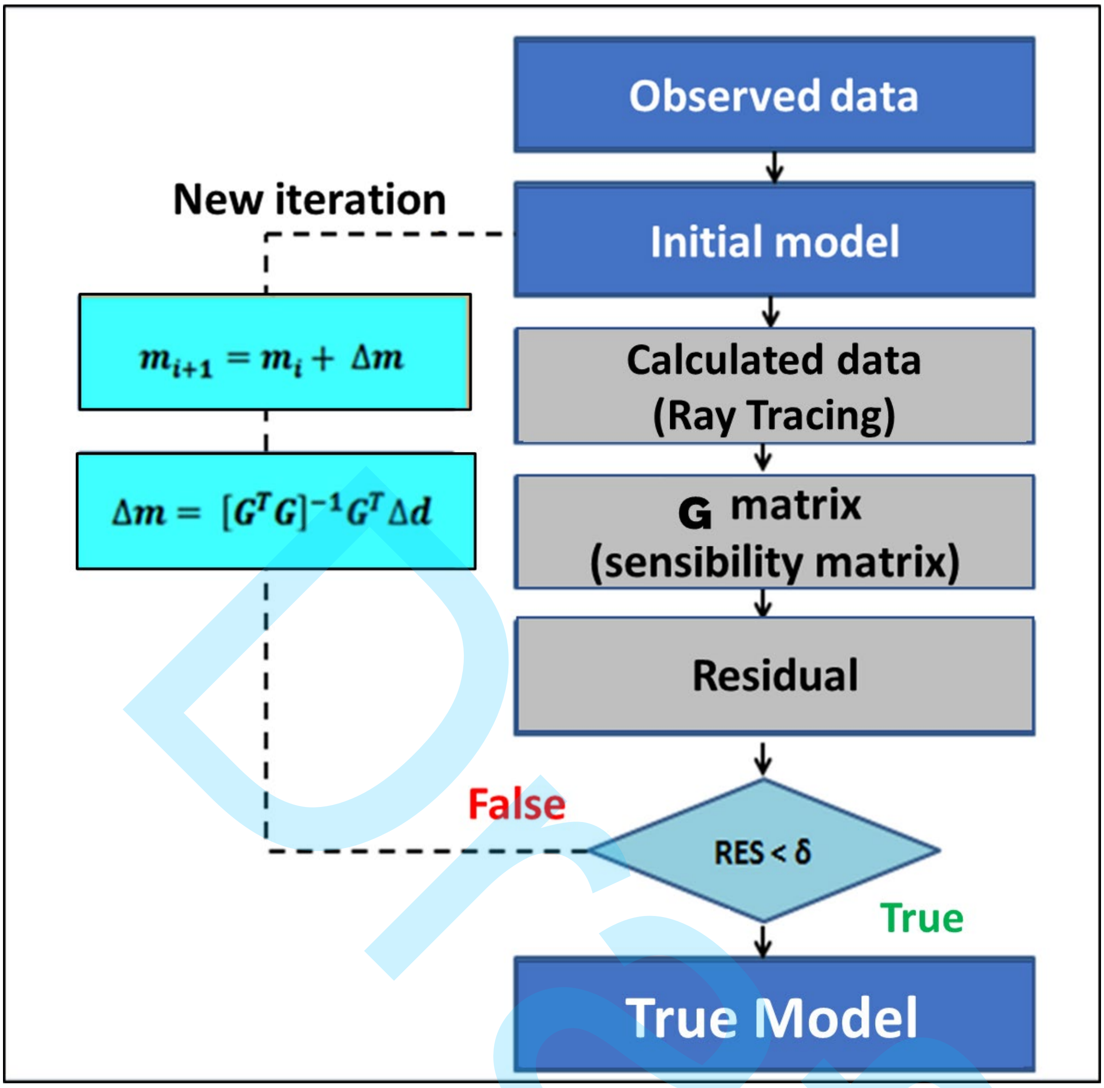


**Figure 4 –** General workflow of seismic tomographic inversion. Adapted from Carbonesi (2018).

Minimizing Equation 2 means looking for the solution with the smallest possible residue to the observed data and obtaining the parameters that best fit the observations. It must find the points at which your derivative is zero to minimize the objective function. Thus, by deriving Equation 2 and equaling to zero, one obtains

$$\boldsymbol{m} = [\boldsymbol{G}^T\boldsymbol{G}]^{-1}\boldsymbol{G}^T\boldsymbol{d} \qquad \text{Eq. 3}$$

Substituting **m** for **Δm** and **d** for **Δd,** gives:

$$\Delta\boldsymbol{m} = [\boldsymbol{G}^T\boldsymbol{G}]^{-1}\boldsymbol{G}^T\Delta\boldsymbol{d} \qquad \text{Eq. 4}$$

**Δm** is the velocity model update term and **Δd =**$\|\boldsymbol{d}_{obs} - \boldsymbol{d}_{calc}\|_2{}^2$ . The term depends on the inverse of the $\boldsymbol{G}^T\boldsymbol{G}$ matrix. In Equation 5, the updated model $\boldsymbol{m}_{i+1}$

$$\boldsymbol{m}_{i+1} = \boldsymbol{m}_i + \Delta\boldsymbol{m} \qquad \text{Eq. 5}$$

The tomographic process will run a number of predefined iterations is reached or when the residue is less than the stipulated value is expressed by:

$$\|\boldsymbol{d} - \boldsymbol{G}\boldsymbol{m_s}\|_2 < \delta \quad \text{Eq. 6}$$

Where:

$\boldsymbol{m_s}$ is a solution to the inverse problem modeled by $\boldsymbol{G}$ that satisfies the condition;
$\boldsymbol{Gm_s}$ is the predicted data, with the result of the inversion;
$\|\boldsymbol{d} - \boldsymbol{Gm_s}\|_2$ it is the norm of the error between the observed data and the predicted data; and $\delta$ is the value chosen as a tolerance for the error norm between the observed data and the predicted data.

Another point is related to the methods of minimizing a problem. The starting point, in the case of tomography in some cases, is the initial velocity model, which must be close enough to the solution for the problem to converge. If this aspect not ensured, there is the possibility of moving away from the "real" solution to the problem, finding a local minimum of the function; the updated model $\boldsymbol{m_{i+1}} = \boldsymbol{m_i} + \left[\boldsymbol{G}^T\boldsymbol{G}\right]^{-1}\boldsymbol{G}^T\Delta\boldsymbol{d}$ process will end, but it is still far from the actual model that is found in the subsurface (Figure 5). In other cases, it can even be forcibly stopped by not converging to any minimum, nor local, much less global (Figure 6).

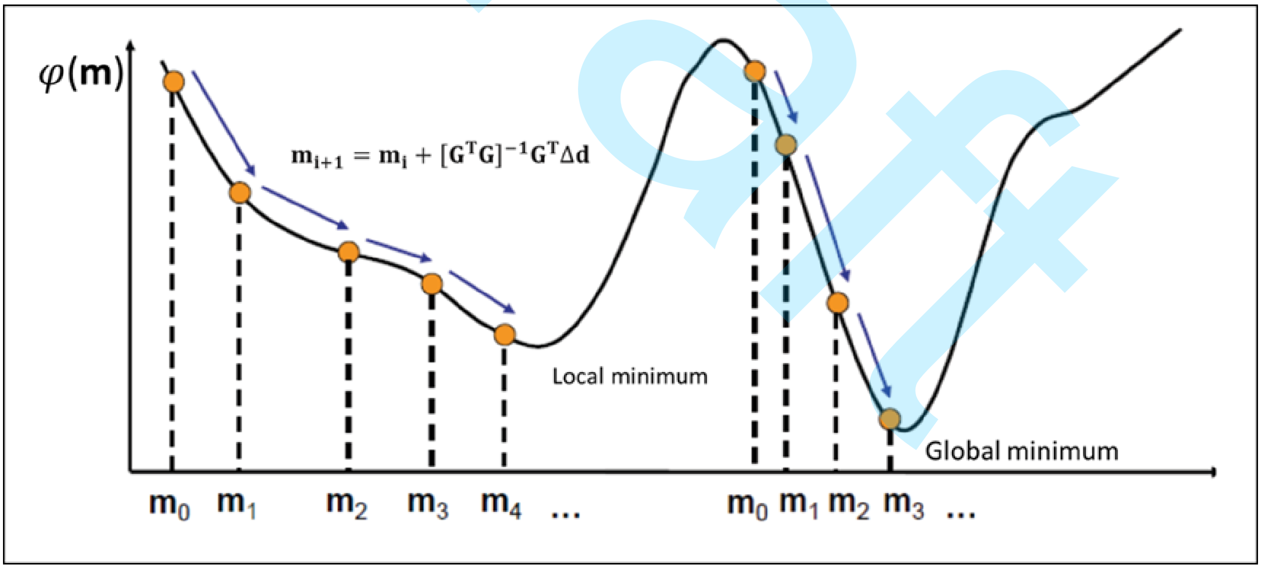


**Figure 5 -** Graphical representation of the objective function in relation to property models. Adapted from Soares Filho (2018).

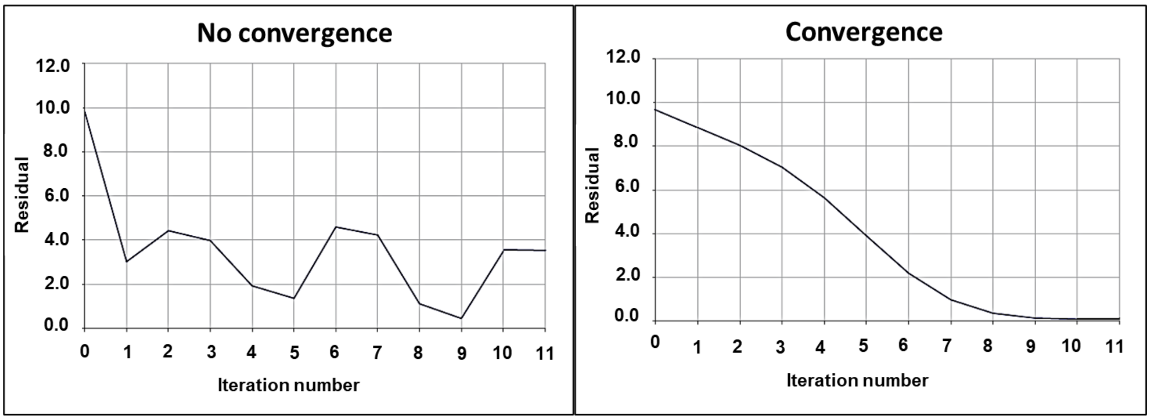


**Figure 6 –** Examples of graphs illustrating the objective function versus iteration for no convergence and convergence cases. Adapted from Santos (2018).

Most geophysical studies resolve inverse problems since acquiring direct measurements of physical properties is costly. In addition, direct measurements are restricted to spatially limited areas and difficult to extrapolate to the entire area of interest with the necessary accuracy, even with the use of geostatistical methods.

According to Zhdanov (2002), Tikhonov's work demonstrates that ill-posed problems can be solved mathematically. A solution is to be stable if slight variations in the values of **d** lead to minor changes. If that does not happen, you have an unstable solution. Defining it more rigorously, operator $\mathbf{G}^{-1}$ (inverse of **G**) is to be continuous when it presents stability for the entire space of solutions (Muniz, 1999). With the continuous $\mathbf{G}^{-1}$ operator in this set, it is necessary to know a priori that a solution is contained in a subset of all possible solutions. When this subset is selected, the ill-posed problem becomes conditionally well-posed.

In the case of some indeterminate linear systems (with several unknowns below the number of equations), a studied solution was to approach the minimum norm's least squares. That is, an additional term is associated with the quadratic discrepancy term. This can be generalized to solve ill-posed problems, and it is necessary to provide additional information. The regularization method determines the smoothest approximate solution and checks its compatibility with the observed data for a given noise level.

The purpose of regularization techniques is to make the operator who inverts the data continuously equivalent to making the solutions stable and the problem well-posed. When regularizing the inversion, the problem to be solved is no longer precisely the original problem and becomes a problem that approaches the original (Figure 7). The smoothing factor (or parameter) $\lambda$ determines the weight given to smoothing in the inversion process, and according to $\lambda$ tends to 0, the smoothed solution ($\mathbf{m}\lambda$) must tend asymptotically to the correct solution $\mathbf{m_c}$ (Zhdanov, 2002), as well as the smoothed operator must tend to the $\mathbf{G}^{-1}$ operator.

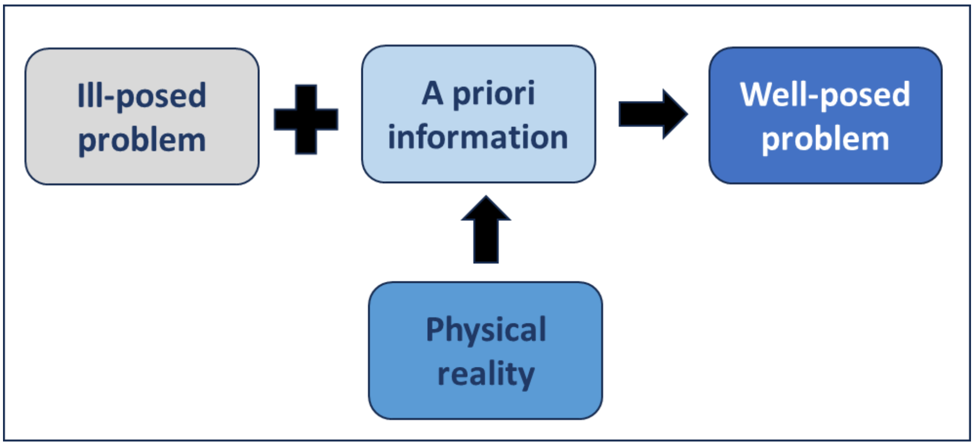


**Figure 7** - Schematic representation to transform an ill-posed problem into a well-posed problem. Adapted from Velho (2008).

The solution of the inverse problem without regularization is the minimization of $\|\boldsymbol{d} - \boldsymbol{G}\boldsymbol{m}_s\|_2$, called objective function is given by:

$$\min \|\boldsymbol{d} - \boldsymbol{G}\boldsymbol{m}_s\|_2 \quad \text{Eq. 7}$$

To obtain a general expression that is minimized, simply apply Lagrange multipliers to the given condition, the result of which is:

$$\min \|\boldsymbol{d} - \boldsymbol{G}\boldsymbol{m}_s\|^2{}_2 + \lambda^2 \|\boldsymbol{m}_s\|^2{}_2 \quad \text{Eq. 8}$$

The higher-order Tikhonov regularizations follow the same logic as zero-order regularization, just replacing the minimization of the $\mathbf{m_s}$ norm by minimizing an $\mathbf{m_s}$ function given by:

$$\min \|\boldsymbol{d} - \boldsymbol{G}\boldsymbol{m}_s\|^2{}_2 + \lambda^2 \|\boldsymbol{L}\boldsymbol{m}_s\|^2{}_2 \quad \text{Eq. 9}$$

Where:

**L** is the matrix of the operator considered (derived first or second from $\mathbf{m_s}$).

The Tikhonov regularization of order 1 uses the first derivative of $\mathbf{m_s}$ and the regularization of order 2, the second derivative are given by equations:

$$\boldsymbol{L}^{(1)}\boldsymbol{m}_s(x,z) = \left(\frac{\partial \boldsymbol{m}_s(x,z)}{\partial x} + \frac{\partial \boldsymbol{m}_s(x,z)}{\partial z}\right) \quad \text{Eq. 10}$$

$$\boldsymbol{L}^{(2)}\boldsymbol{m}_s(x,z) = \left(\frac{\partial^2 \boldsymbol{m}_s(x,z)}{\partial x^2} + \frac{\partial^2 \boldsymbol{m}_s(x,z)}{\partial z^2}\right) \quad \text{Eq. 11}$$

If the matrix **L** is considered as the identity matrix, it is the zero-order regularization.

This study examines the impact of regularization on refraction tomography. The study area represents a coastal environment near South Boston, Massachusetts (Zhang and Toksöz,1998), a shallow-structure 2-D velocity model. The acquisition geometry for parameterization of the forward modeling is defined as the interval between shooting points in 40 m, the total number of shots in 176, the depth of sources and receivers in 20 m, the interval between receivers in 10 m, and the total number of receivers in 150 and the real velocity model and the acquisition geometry, which are represents in Figure 8. The model contains three layers and a seabed channel structure, with velocities of 1,500 m/s (water), 2,000 m/s, and 2,500 m/s. In addition, the velocity model consists of 250 cells in the horizontal direction and 25 cells in the vertical direction (depth) with a uniform spacing of 10 m. Besides, it was added a white noise (gaussian distribution) for forward modeling data. The white noise has a value obtained by the pseudorandom drawing of a number according to a gaussian distribution with a standard deviation equal to the value expected for the error in obtaining the first arrival time (Almeida, 2013).

In the study, the process ends when the residual is less than $\delta = 1.0 \times 10^{-8}$ ms or when it reaches a maximum number of iterations, n=40. The actual model was compared with travel time tomography results without regularization using Tikhonov's regularization schemes. Travel times for tomography were obtained by forward modeling this model using the same tomography algorithm to calculate travel time.

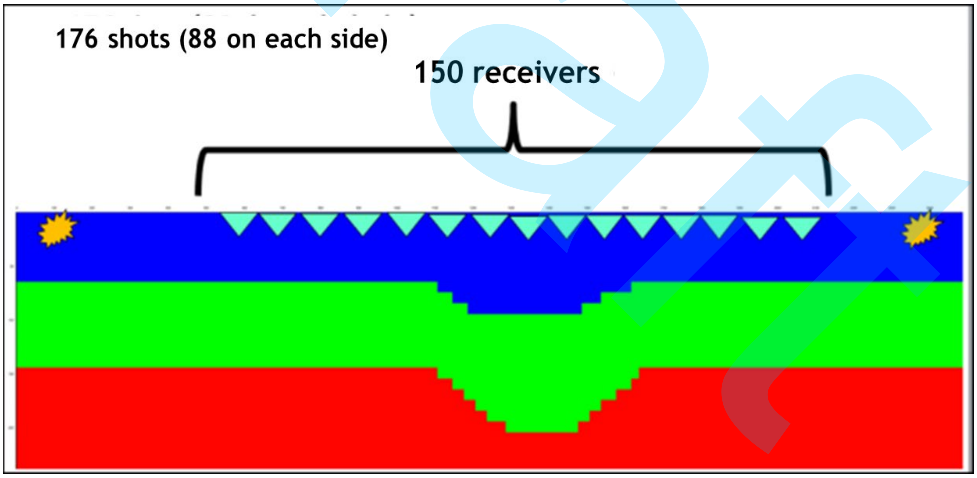


**Figure 8 -** Representation of the real velocity model and the acquisition geometry. Adapted from Bulhões (2020).

Figure 9 shows the initial velocity model used for tomographic inversion, consisting of two flat, parallel, and horizontal layers with velocities of 1,500 m/s and 2,500 m/s. The true velocity model (Figure 9a) is represented by the model resulting from the refraction tomography without applying the regularization (Figure 9b).

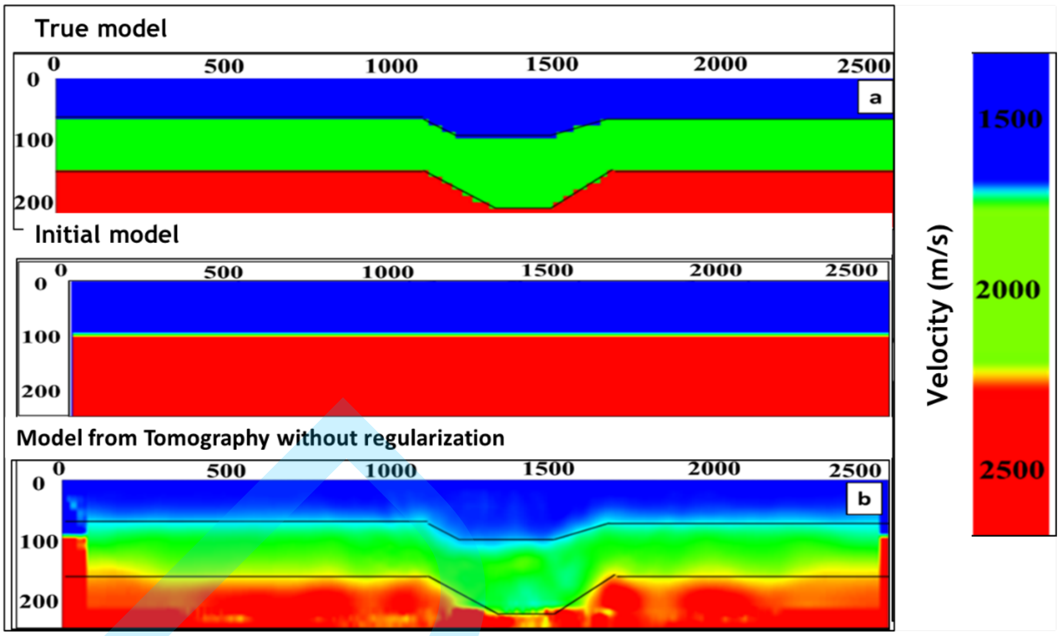


**Figure 9 -** True velocity model, initial model input for refraction tomography and tomography result without regularization.

Figure 10 shows the residual of the tomographic process as a function of the iteration. The axis referring to the residue is in the logarithmic scale at base 10. This graph observes that the convergence of the tomographic inversion occurs from iteration 28.

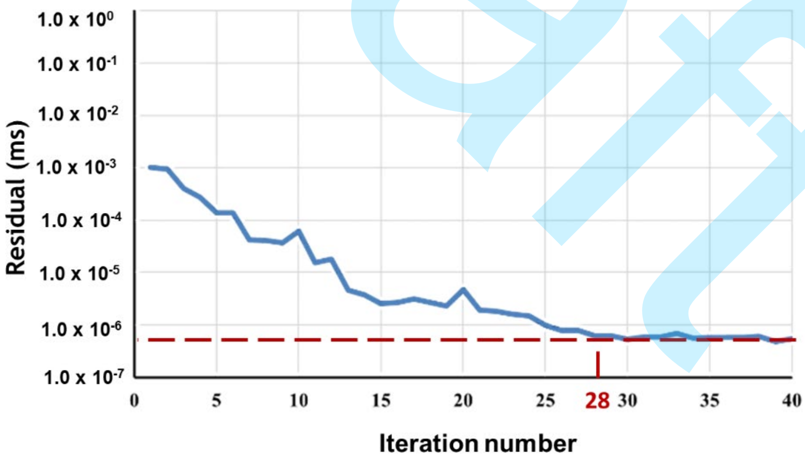


**Figure 10 -** Variation of the residual of the tomographic inversion without regularization according to the iteration.

The effects of regularization are analyzed through a sensitivity study based on the regularization parameters, which impact the algorithm's convergence and stability and the resulting model. The stability and convergence are also analyzed using graphs of the behavior of the residue as a function of iteration. Stability does not guarantee convergence in a tomographic inversion, a nonlinear process. However, the stability presence of the method favors obtaining a converged solution. On the other hand, the higher regularization parameter λ gives more weight to the regularization term, leading to a smoother but potentially less accurate solution that is less sensitive to noise. The smoothing effect of the regularization term minimizes the impact of noisy data on the final solution, leading to a more stable and reliable inversion.

### Tikhonov Regularization Procedure

The analysis of the regularization effect on refraction tomography utilizes programs developed by the Seismic Imaging Group of Universidade Federal Fluminense (GISIS-UFF). These programs are grounded in the work of Almeida (2013) and further complemented by Bulhões (2020). The tomography program effectively derives the transit time matrix by employing the ray tracing technique established by Podvin and Lecomte (1991). It achieves this through finite differences applied to the eikonal equation, allowing for the calculation of first arrivals and constructing a tomographic matrix with regularization. To enhance the results, Tikhonov regularizations of both first and second order are implemented. Specifically, three strategies are utilized for first-order regularization: (i) conventional methods derived in both horizontal and vertical directions, (ii) derivatives focused solely on the horizontal component, and (iii) derivatives enhanced with an advanced scheme. This comprehensive approach enables the application of tomographic inversion for regularization parameter values that range from $1.0 \times 10^{-8}$ to $1.0 \times 10^{3}$.

In the context of first-order Tikhonov regularization, the stabilization of the inverse problem is achieved by incorporating the first derivative in the x and z directions (and y in the three-dimensional case), as articulated in Equation 10. Furthermore, the second regularization approach modifies this first-order approach by utilizing only the horizontal component of the operator derived, thereby streamlining the process. Lastly, the study adopts Tikhonov regularization of the second order, which involves applying the second derivative of the model across the spatial dimensions, as indicated by Equation 11. These methodologies collectively contribute to a more robust understanding of the impact of regularization on refraction tomography, paving the way for enhanced seismic imaging and analysis.

## RESULTS AND DISCUSSION

The graphs in Figure 11 show the residuals of transit times as a function of the iteration for the different regularization parameters. The strategy for choosing Tikhonov's regularization parameters was based on the work of Santos and Bassrei (2007). This approach involved choosing different orders of magnitude to observe the tomography's response in relation to the regularizing parameter.

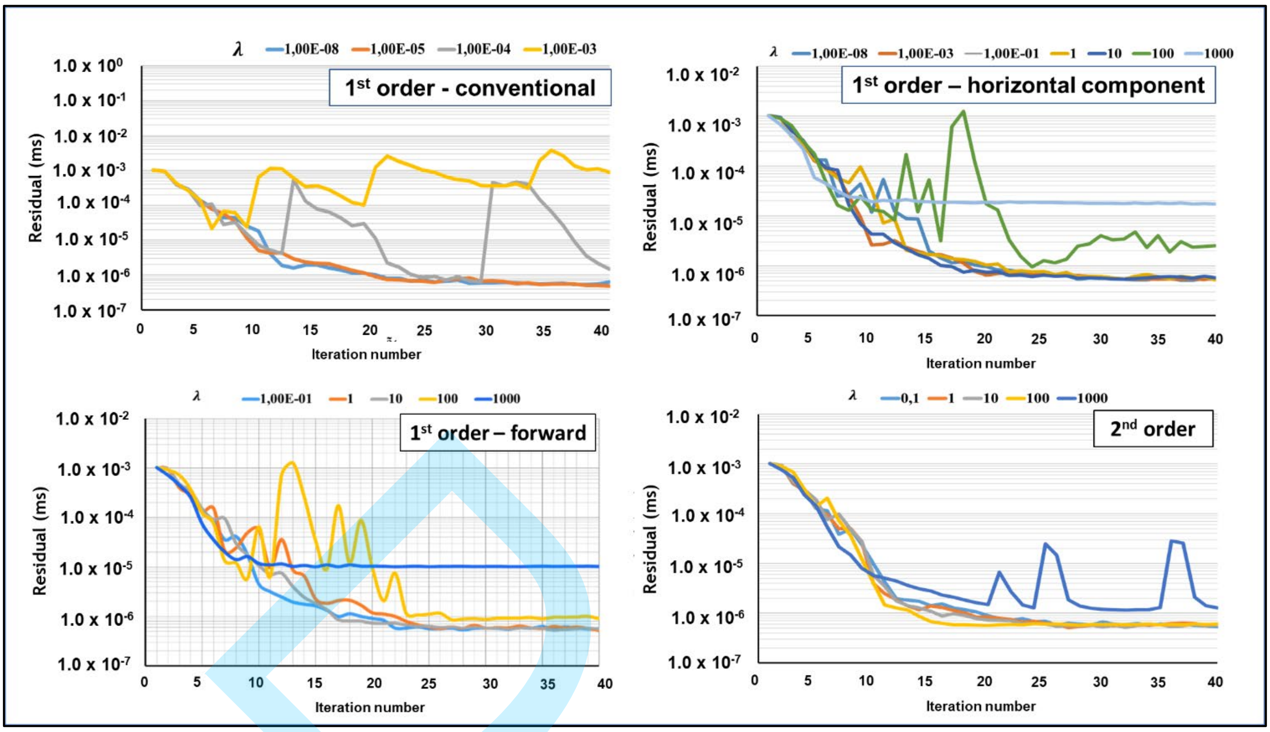


**Figure 11 -** Evolution of travel time residual as a function of tomography iteration using Tikhonov regularization for each scenario: first-order (conventional, horizontal component and forward) and second-order.

Significant instability arises in the case of Tikhonov regularization of order 1 when values exceed 1.0 x $10^{-5}$. Specifically, the errors amplify during the iterative process of the tomographic algorithm. When applying order 1 horizontal component regularization, we observe numerical instability at the parameter λ = 1.0 x $10^{-1}$. Moreover, using λ values greater than 1.0 x $10^{2}$ results in residual convergence for values higher than those previously tested. This convergence suggests that the objective function has reached a local minimum. When λ is set to 1.0 x $10^{1}$ or 1.0 x $10^{-3}$, convergence occurs in fewer iterations, as the residual values are closer during the tomographic inversion steps.

Furthermore, during iterations 9 to 24 of the first-order regularization using an advanced scheme, we experience numerical instability at λ = 1.0 x $10^{2}$, where convergence hovers around 1.0 x $10^{-6}$. However, for values lower than 1.0 x $10^{2}$, the process advances smoothly without sudden fluctuations, with residuals converging to approximately 6.0 x $10^{-7}$. Notably, for λ = 1.0 x $10^{3}$, the residual converges to 1.0 x $10^{-5}$ starting from the 10th iteration, indicating that the model has achieved a local minimum. In the scenario of second-order regularization, we encounter numerical instability at λ = 1.0 x $10^{3}$ during the tomographic process. Nonetheless, for values below 1.0 x $10^{3}$, the procedure progresses smoothly without abrupt changes, resulting in residuals converging to around 6.0 x $10^{-7}$.

Obtaining optimal values for regularization is not straightforward; however, strategies such as the L-curve are instrumental in guiding our choices. The L-curve represents a plot of the regularized solution's size against and corresponding residual's size for all valid regularization parameters (Hansen, 1992; Hansen and O'Leary, 1993).

Although the L-curve may lack predictive power, it is a valuable tool for identifying the best-fit parameters from the results of tomographic inversions, different from those reported by Santos and Bassrei (2007). It is essential to recognize that each physical problem presents its optimal regularization parameter based on the magnitude of the modeled property. Among the various tested regularization cases, the optimal λ parameters for each scenario are located at the peak of the residue curve. This curve, a function of the parameter λ, aids in determining the ideal value for each scenario. For a more precise understanding, Figure 12 illustrates the RMS residue of the transit times as a function of the parameters, highlighting this important relationship. The knee of the L-curve illustrates a trade-off between smoother solutions, which may have higher errors, and rougher solutions, which typically feature more minor errors. Consequently, detecting the knee provides a heuristic criterion for selecting the most appropriate solution. Solutions near the curve's knee are also considered acceptable and potentially more physically meaningful. This approach enables us to achieve a solution that satisfies error minimization criteria, smoothness, and physical interpretability. As a result, visual inspection of the L-curve and manual detection of its knee become necessary to select the best regularization parameter.

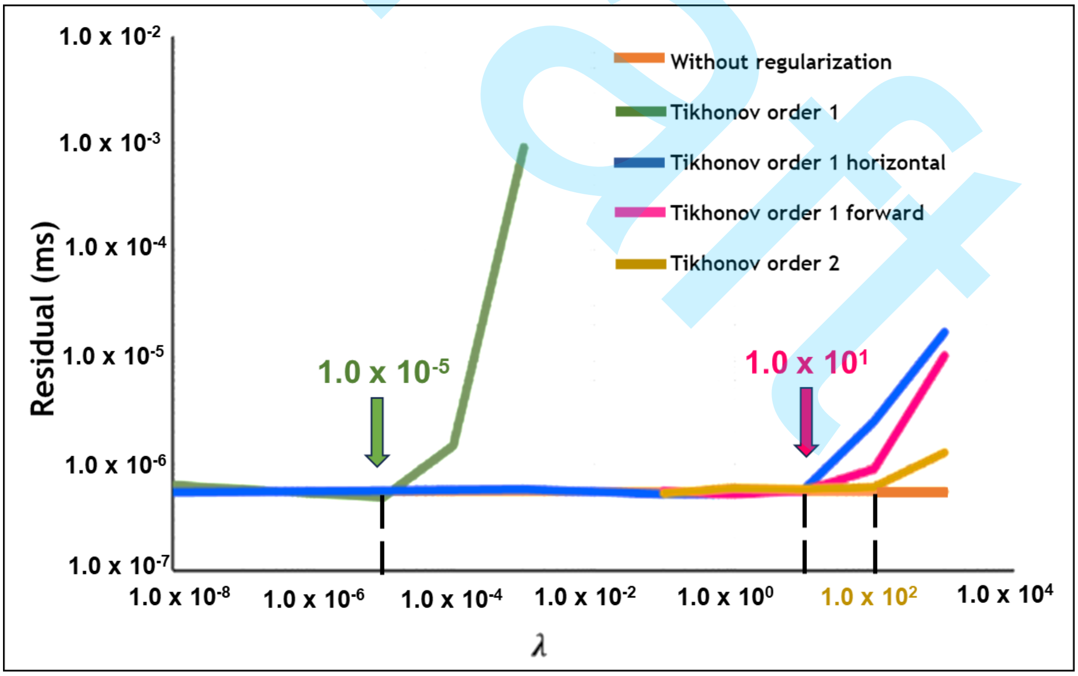


**Figure 12** - RMS residue of travel time as a function of regularization parameters λ for each scenario.

Figure 13 illustrates the variation of the RMS residue in transit time as a function of the iteration for the respective optimal values while also providing a comparison with tomography that lacks regularization. Notably, tomography without regularization converges after 31 iterations. In contrast, when employing regularization, we observe a significant improvement in convergence: it occurs at iteration 22 for order 1; 25 for order 1 horizontal component; 28 for order 1 forward; and impressively at just 17 iterations for order 2. This evidence strongly suggests that regularization enhances the efficiency of the tomographic process, leading to faster convergence and, ultimately, better results.

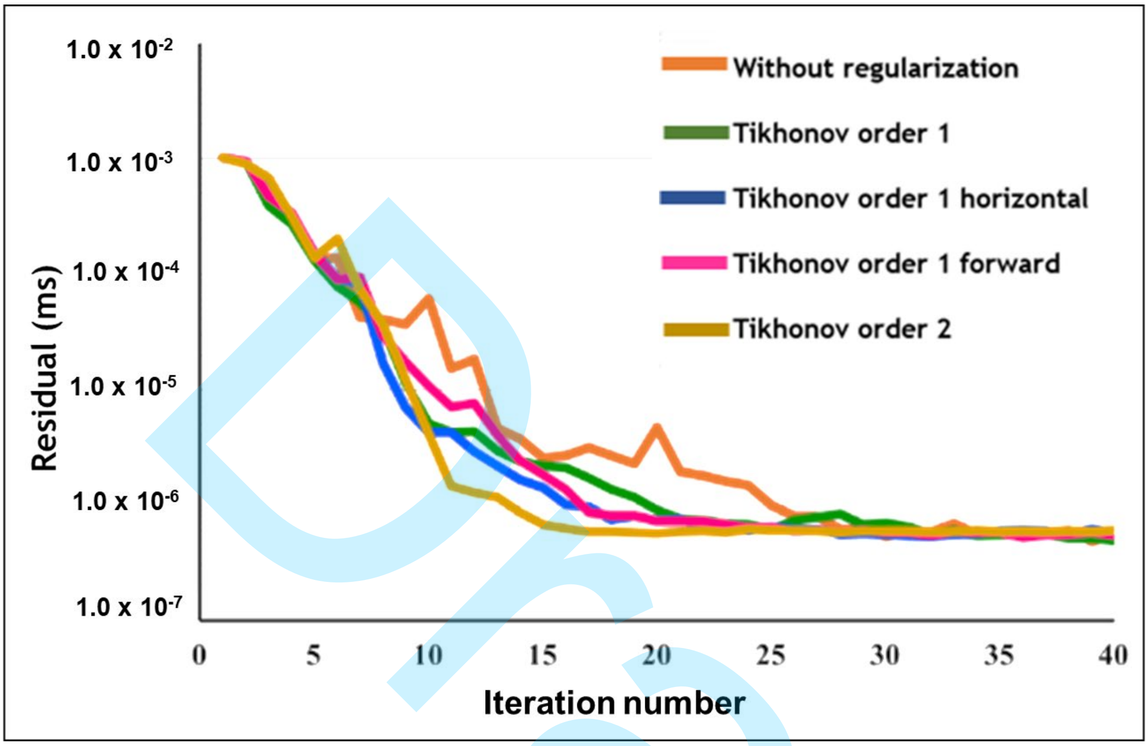


**Figure 13** - RMS residue of travel time as a function of iteration for cases with regularization (first and second order) and without regularization.

Figure 14 shows the actual models alongside the tomographic results without regularization, utilizing the optimal parameterization values. It is important to note that the lack of regularization leads to distorted structures, as illustrated in Figure 14b. Similarly, we see the same distortion in cases involving order 1 regularization, depicted in Figure 14c. In contrast, the results for the order 1 horizontal component (Figure 14d), the forward order 1 (Figure 14e), and the order 2 method (Figure 14f) demonstrate a significant improvement; these cases do not exhibit any distortion in the structures. Notably, the second-order Tikhonov regularization achieves the best results, according to the findings presented by Denisov et al. (2006) and Teimoornega and Poroohan (2010). The second-order Tikhonov method offers superior feature delineation in both studies compared to order 1, thereby highlighting the advantages of utilizing higher-order regularization in tomographic applications.

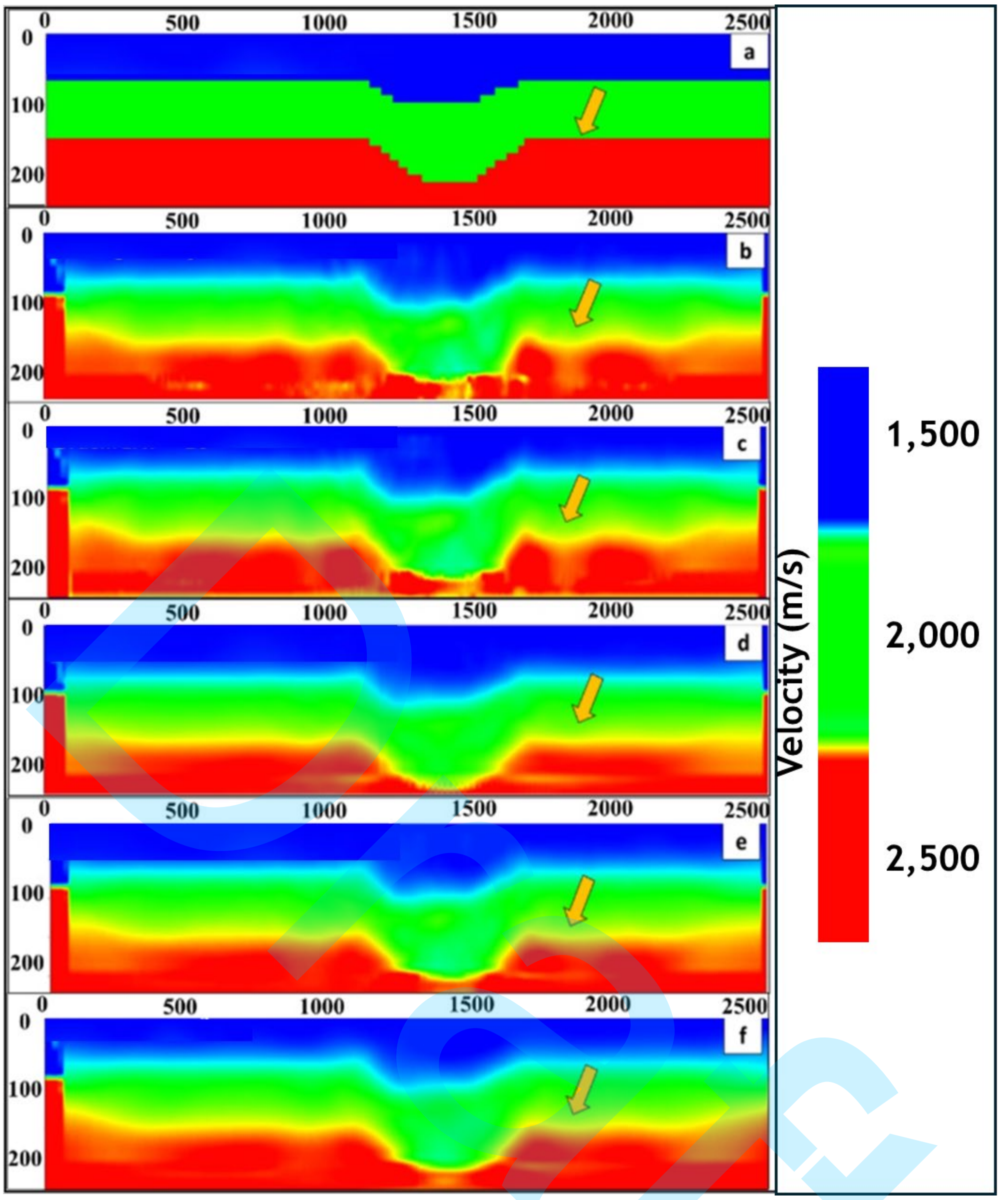


**Figure 14 -** (a) True velocity model, (b) Tomography without regularization, Tikhonov regularization (c) order 1, (d) order 1 horizontal component, (e) order 1 forward scheme and (f) order 2.

Table 1 shows the summary of the tested regularizations and the individual results after the 40 iterations of the tomographic process. Table 1 describes the optimal value of the parameter λ for Tikhonov regularization; the step in which the inversion begins to converge to the respective parameter λ and the RMS residue of the travel time compared to the actual data, δt means the RMS difference with travel time observed and travel time calculated ($\|\boldsymbol{d_{obs}} - \boldsymbol{d_{calc}}\|_2$ ).

Tikhonov regularizations of order 2 converge the tomographic process faster from step 17. In the case of conventional Tikhonov regularization of order 1, it is verified that its use, in addition to making the tomographic process slower to converge than without regularization, goes from 28 to 31 steps.

**Table 1**: Summary of the regularizations applied with the respective waste statistics in the 40th iteration.

| Regularization schemes | λ optimum | Iteration number convergence | RMS δt |
|---|---|---|---|
| Without regularization | - | 28 | $5.47 \times 10^{-7}$ |
| Tikhonov 1st order | $1.0 \times 10^{-5}$ | 31 | $4.88 \times 10^{-7}$ |
| Tikhonov 1st order horizontal | $1.0 \times 10^{1}$ | 22 | $5.76 \times 10^{-7}$ |
| Tikhonov 1st order forward | $1.0 \times 10^{1}$ | 25 | $5.54 \times 10^{-7}$ |
| Tikhonov 2nd order | $1.0 \times 10^{2}$ | 17 | $6.06 \times 10^{-7}$ |

## Tikhonov regularization limitations

Tikhonov regularization methods are widely used but also have certain limitations. One significant limitation observed in this work is determining the regularization parameter, λ, which controls the regularization level. When λ is too small, the solution is insufficiently regularized, resulting in instability and oscillations. The graphs in Figure 11 illustrate these instabilities for these regularizations. On the other hand, if λ is too large, the solution becomes overly smooth, potentially losing critical details.

Additionally, the choice of the regularization operator can be arbitrary and highly dependent on the specific problem, which can lead to suboptimal solutions. The parameter λ determines the significance of the regularization constraint relative to the problem residual.

Thus, we observe which the choice an inappropriate λ can jeopardize the accuracy of the solution. To address this, methods such as cross-validation assist in finding a value of λ that effectively balances solution accuracy with stability. Moreover, the regularization operator, such as the Tikhonov L-matrix, significantly influences the nature of the solution.

Choosing an unsuitable operator can result in either over- or under-regularization. While Tikhonov regularization is often applied to linear problems, its extension to nonlinear problems introduces additional complexity, necessitating adaptations and further analysis. Importantly, in some cases, Tikhonov methods require prior knowledge about the problem, such as the operator's structure or the properties of the solution. Consequently, Tikhonov regularization may not be the most suitable approach for all types of problems, particularly when total variation (TV) regularization could be more effective, as seen in applications like image inpainting.

## CONCLUSIONS

This study evaluates the effects of regularization on shallow-surface seismic refraction tomography and its influence on the resulting seismic velocities. Notably, the analysis highlights that regularization alone cannot solve ill-posed problems. Using inadequate regularization or parameter values fails to enhance the tomography results. Consequently, our sensitivity study employing Tikhonov regularizations reveals distortions in geological structures due to inappropriate choices of regularization parameters. Moreover, the velocity model generated through classical first-order regularization, derived specifically in the x and z directions, does not resolve issues seen without regularization and demonstrates significant numerical instability.

In contrast, applying first-order regularization with horizontal derivatives leads to velocity models that closely align with the true model, showing less structural distortion than classical first-order regularization. Notably, the Tikhonov parameter that optimally stabilizes the tomographic inversion and minimizes structural distortions is $\lambda=1.0 \times 10^1$. Additionally, the first-order Tikhonov regularization with a progressive scheme yield results akin to the first order of the horizontal component, affirming that $\lambda=1.0 \times 10^1$ optimizes numerical stability and structural accuracy. Moreover, refraction tomography utilizing second-order Tikhonov regularization converges faster than its counterparts, achieving results within 17 iterations. With a $\lambda$ value of $1.0 \times 10^2$, this approach produces a velocity model with minimal structural distortions. While the first-order scenario with a horizontal derivative delivers the best overall results, its convergence is notably slower, completing in 28 iterations. Convergence plays a critical role in tomographic processes, where results may be similar yet can vary in the degree of smoothing. This aspect aligns with the objective of seismic tomography: enhancing seismic processing about the initial model, which ultimately feeds into seismic imaging and Full-Waveform Inversion (FWI) algorithms. Among the four application scenarios of Tikhonov regularization, the best outcomes are consistently observed in the second order, first-order horizontal component, and first-order with progressive schemes. This convergence speed is particularly significant in the oil and gas industry, where seismic data volume continues to increase, making processing time a vital variable. As a result, the second-order approach demonstrates superior convergence with fewer iterations, yielding one of the lowest RMS errors at a speed of 126.87 m/s. Our findings reinforce those of Denisov et al. (2006) and Teimoornega and Poroohan (2010), indicating that second order Tikhonov regularizers provide better feature delineation than first-order methods. This position is second order regularization as a powerful tool in pursuing accurate seismic imaging.

Looking ahead, several perspectives for future work emerge: first, testing other regularization methods for refraction tomography to evaluate their efficiency, particularly Total Variation and Modified Total Variation; second, assessing how effectively the models obtained from refraction tomography can serve as initial models for Full-Waveform Inversion (FWI). Additionally, we intend to apply the tomographic inversion program to real data from onshore and shallow marine environments. This approach will undoubtedly enhance our understanding and advance the field.

## ACKNOWLEDGMENTS

The authors thank Petrobras and the Universidade Federal Fluminense for allowing the publication of this work. The first author thanks Bruna Faustino for their help and partnership, and colleagues Alexandre Maul, Bruno Dias, Rogério Santos and Roger Matsumoto.

## REFERENCES

ALMEIDA VTX. 2013.Tomografia sísmica de superfície: modelagem direta calculando as trajetórias de ondas refratadas. Master Dissertation. Universidade Federal Fluminense. Niterói, RJ, Brazil.

ASTER RC, BORCHERS B and THURBER CH. 2005. Parameter Estimation and Inverse Problems. Elsevier Academic Press. 320– p.

BEGNAUD ML, MYERS SC, BALLARD S, RAMIREZ AL, PASYANOS ME and PHILLIPS WS. 2013. Regional Seismic Travel Time (RSTT) Tomography. American Geophysical Union, Spring Meeting 2013, abstract id. S33C-01. Available on: https://www.ctbto.org/fileadmin/user_upload/SnT2013/Slides/Thursday/T1-O16_Begnaud.pdf

BEJARANO SL and BASSREI A. 2016. Critique of solutions in linearized inverse problems: Numerical experiments in traveltime tomography. Revista Brasileira de Geofısica (2016) 34(4): 495-508 Available on: https://doi.org/10.22564/rbgf.v34i4.871

BIANCO E. 2013. Backwards and forwards reasoning. In blog Agile. Posted 16-April-2013. Available on: https://agilescientific.com/blog/2013/4/16/backwards-and-forwards-reasoning.html

BULHÕES, FC. 2020. Efeitos da Regularização na Tomografia de Refração. Master Dissertation. Universidade Federal Fluminense. Niterói, RJ, Brazil. 2020.

BULHÕES FC and SANTOS LA. 2022. A evolução do método sísmico usando análise bibliométrica. In: IX Simpósio Brasileiro de Geofísica. SBGf: Curitiba, Brazil. 2022.

BULHÕES FC, AMORIM GAS, BRUNO VLVR, FERREIRA, GD, PEREIRA, ES and CASTRO RF. 2014. Fluxo para Construção do Modelo de Velocidade Regional da Bacia de Campos. In: VI Simpósio Brasileiro de Geofísica. SBGf: Porto Alegre, Brazil. 2014. https://doi.org/10.22564/6simbgf2014.082.

BULHÕES FC, FERREIRA GD and CAPARICA JR., JF. 2018. Impacts of Seismic Velocity Model Calibration for Time-Depth Conversion: A Case Study. Brazilian Journal of Geophysics, 36(4), 401-410. https://doi.org/10.22564/rbgf.v36i4.1965.

CARBONESI BL. Tomografia de Refração e sua Aplicação na Identificação dos Altos Estruturais do Gráben da Casa de Pedra, RJ. Undergraduate Final Project. Universidade Federal Fluminense. Niterói, RJ, Brazil. 2018.

CLAERBOUT JF and MUIR F. 1973. Robust modeling with erratic data. Geophysics, 38(5), p. 826–844. https://doi.org/10.1190/1.1440378.

DENISOV AM, KRYLOV AS and SIBANOV VN. 2006. Second Order Tikhonov Regularization Method for Image Filtering. In: International Conference Graphicon 2006, ICM&MG SB RAS: Novosibirsk Akademgorodok, Russia, 2006.

DOBECKI TL and ROMIG PR. 1985. Geotechnical and groundwater geophysics: Geophysics, v.

50, n. 12, p. 2621-2636. https://doi.org/10.1190/1.1441887

FERZIGER, J.H., and PERIĆ, M. 1996. Computational Methods for Fluid Dynamics. Springer-Verlag. Berlin Heidelberg. 356 pp. https://doi.org/10.1007/978-3-642-97651-3.

HADAMARD J. 1902. Sur les problèmes aux dérivées partielles et leur signification physique. Princeton University Bulletin. 13, 49–52

HANSEN PC. 1992. Analysis of discrete ill-posed problems by means of the L-curve, SIAM Review 34, 4, 561–580. https://doi.org/10.1137/1034115

HANSEN PC and O'LEARY DP. 1993, The use of the L-curve in the regularization of discrete ill-posed problems, SIAM J. Sci. Comput. 14 (6), 1487–1503. https://doi.org/10.1137/0914086

HEATH MT., 2002, Scientific Computing: An Introductory Survey. 2nd ed. McGraw-Hill. 563 pp.

IVANOV VK. 1962, On linear problems which are not well-posed. Sov. Math., Dokl. 3, 981–983. [English translation from the Russian original: Dokl. Akad. Nauk, 145, 2, 270–272].

IVANOV J, MILLER RD, XIA J, STEEPLES D and PARK CB. 2005a. Joint analysis of refractions with surface waves: An inverse solution to the refraction-traveltime problem. Geophysics, Society of Exploration Geophysicists, v. 71, n. 6, p. R131–R138, http://dx.doi.org/10.1190/1.2360226.

IVANOV J, MILLER RD, XIA J, STEEPLES D and PARK CB. 2005b. The inverse problem of refraction travel times, part I: Types of geophysical nonuniqueness through minimization. Pure and Applied Geophysics, Birkhäuser-Verlag, v. 162, n. 3, p. 447–459–,http://dx.doi.org/10.1007/s00024-004-2615-1.

LI SZ and JAIN A. 2009. L2 norm. In: Encyclopedia of Biometrics. Springer, Boston, MA. https://doi.org/10.1007/978-0-387-73003-5_1070

LINES L and NEWRICK R. 2004. Fundamentals of Geophysical Interpretation. Society of Exploration Geophysicists. 288 p. http://dx.doi.org/10.1190/1.9781560801726.

MAUL A, FEILHABER M and GONÇALVES, PA. 2005. Modelagem Geológica de Velocidades Sísmicas Utilizando o GoCad. Petrobras Internal Material.

MAUL A, FONSECA J, TEIXEIRA L, BARROS P, BOECHAT J, NUNES JP, YAMAMOTO T, GONZÁLEZ M and GONZÁLEZ G. 2018. Modelling intra-salt layers when building velocity models for depth migration Examples of the Santos Basins, Brazilian offshore. In: 88th Annual Meeting. Anaheim – CA, USA. SEG Technical Program Expanded Abstracts 2018, p. 3764–3767. http://doi: 10.1190/segam2018-2996209.1.

MENKE W. 1989. Geophysical Data Analysis: Discrete Inverse Theory: revised edition, Academic Press, Elsevier. 289 pp.

MENKE W., 2012, Geophysical data analysis: Discrete inverse theory, 3rd ed., Academic Press. 330 pp

MUNIZ WB. 1999. Um Problema Inverso em Condução do Calor utilizando Métodos de Regularização. 1999. 79P. Master Dissertation in Mathematics. Instituto de Matemática - Universidade Federal do Rio Grande do Sul. Porto Alegre, RS, Brazil. 1999.

PHILLIPS DL. 1962 A technique for the numerical solution of certain integral equations of the first kind: Journal of the ACM, 9(1), 84–97. https://doi.org/10.1145/321105.321114.

PODVIN P and LECOMTE I. 1991. Finite difference computation of traveltimes in very contrasted velocity models: a massively parallel approach and its associated tools. Geophysical Journal International. 105, p. 271–284. https://doi.org/10.1111/j.1365-246X.1991.tb03461.x

ROSA ALR. 2018. The Seismic Signal and Its Meaning. Society of Exploration Geophysicists. Geophysical References Series. v. 23. 788 pp. https://doi.org/10.1190/1.9781560803348.

SANTOS LA. 2018. Tomography Applied to Geosciences. [Lecture Notes]. Graduate Program in Ocean and Earth Dynamics, Institute of Geosciences, Universidade Federal Fluminense. Niterói, RJ, Brazil.

SANTOS ETF and BASSREI A. 2007. L- and Θ-curve approaches for the selection of regularization parameter in geophysical diffraction tomography. Computers & Geosciences, 33: 618–629. DOI: 10.1016/j.cageo.2006.08.013

SOARES FILHO DM. 2018. Geophysical Inversion. [Lecture Notes]. Graduate Program in Civil Engineering. Universidade Federal do Rio de Janeiro, Rio de Janeiro, RJ, Brazil.

TANNEHILL JC, ANDERSON DA and PLETCHER RH. 1997. Computational fluid mechanics and heat transfer. 2nd ed. Series in Computational and Physical Processes in Mechanics and Thermal Sciences. 792 pp.

TEIMOORNEGA K and POROOHAN N. 2010. The Application of Discrete Tikhonov Regularization Inverse Problem in Seismic Tomography. Water & Geoscience. In: 4th IASME/WSEAS International Conference on GEOLOGY and SEISMOLOGY (GES '10). World Scientific and Engineering Academy and Society / International Association of Mechanical Engineers, University of Cambridge, UK.

TELFORD W M, GELDART LP and SHERIFF RE 1990. Applied Geophysics. 2nd ed., New York, EUA: Cambridge University Press. 1990. 792p. https://doi.org/10.1017/CBO9781139167932.

TIKHONOV AN. 1963. Solution of incorrectly formulated problems and the regularization method. Sov. Math., Dokl., 5, 1035–1038. [English translation from the Russian original: Dokl. Akad. Nauk, 151, 3, 501–504].

TIKHONOV AN and ARSENIN VY. 1977. Solutions of Ill-Posed Problems, New York, Winston. 258 pp.

TWOMEY S. 1963. On the numerical solution of Fredholm integral equations of the first kind the inversion of the linear system produced by quadrature. Journal of ACM, 10: 97-101. https://doi.org/10.1145/321150.321157

VELHO HFC. 2008. Introdução aos Problemas Inversos: Aplicações em Pesquisa Espacial. Escola de verão em Computação Aplicada – LAC-INPE 2008. Laboratório Associado de Computação e Matemática Aplicada, Instituto Nacional de Pesquisas Espaciais, SP, Brazil.

WOODWARD M, NICHOLS D., ZDRAVEVA O., WHITFIELD, P. and JOHNS, T. 2008. A decade of tomography. Geophysics. 73(5), VE5-VE11. https://doi.org/10.1190/1.2969907.

ZHANG J and TOKSöZ M. 1998. Nonlinear refraction traveltime tomography. Geophysics, 63(5), p. 1726–1737, http://dx.doi.org/10.1190/1.1444468.

ZHDANOV MS. 2002. Tutorial: Regularization in inversion theory: CWP Report: Colorado School of Mines, 136, 47.

**Bulhões, F. C.:** contributed as an Exploration Geophysicist, focusing on the construction of seismic velocity models for time-to-depth conversion on a basin scale. His work has also involved developing and implementing workflows for sensibility analysis for regularization on seismic tomography data; **Santos, L. A.:** contributed as advisor and supervision of the master's research related to this paper; participation in the conceptual and methodological discussions and; review of the scientific content; **Cetale, M.:** contributed through active participation in the conceptual and methodological discussions throughout the development of the study, review of the scientific content and academic supervision of the master's research that formed the basis of this work; **de Almeida, V.T.X.:** contributed as implemented the algorithms for refraction tomography and its regularizations, and review of the scientific content.